

**Marquette University**  
**e-Publications@Marquette**

---

Biomedical Engineering Faculty Research and  
Publications

Biomedical Engineering, Department of

---

9-1-2013

# *Ex Vivo* Diffusion Tensor Imaging of Spinal Cord Injury in Rats of Varying Degrees of Severity

Michael Jirjis  
*Marquette University*

Shekar N. Kurpad  
*Medical College of Wisconsin*

Brian D. Schmit  
*Marquette University, [brian.schmit@marquette.edu](mailto:brian.schmit@marquette.edu)*

---

Published version. *Journal of Neurotrauma*, Vol. 30, No. 18 (September 2013): 1577-1586. [DOI](#). ©  
2013 M.A. Liebert. Used with permission.

# Ex Vivo Diffusion Tensor Imaging of Spinal Cord Injury in Rats of Varying Degrees of Severity

Michael B. Jirjis,<sup>1</sup> Shekar N. Kurpad,<sup>2</sup> and Brian D. Schmit<sup>1</sup>

## Abstract

The aim of this study was to characterize magnetic resonance diffusion tensor imaging (DTI) in proximal regions of the spinal cord following a thoracic spinal cord injury (SCI). Sprague–Dawley rats ( $n=40$ ) were administered a control, mild, moderate, or severe contusion injury at the T8 vertebral level. Six direction diffusion weighted images (DWIs) were collected *ex vivo* along the length of the spinal cord, with an echo/repetition time of 31.6 ms/14 sec and  $b=500$  sec/mm<sup>2</sup>. Diffusion metrics were correlated to hindlimb motor function. Significant differences were found for whole cord region of interest (ROI) drawings for fractional anisotropy (FA), mean diffusivity (MD), longitudinal diffusion coefficient (LD), and radial diffusion coefficient (RD) at each of the cervical levels ( $p<0.01$ ). Motor function correlated with MD in the cervical segments of the spinal cord ( $r^2=0.80$ ). The diffusivity of water significantly decreased throughout “uninjured” portions of the spinal cord following a contusion injury ( $p<0.05$ ). Diffusivity metrics were found to be altered following SCI in both white and gray matter regions. Injury severity was associated with diffusion changes over the entire length of the cord. This study demonstrates that DTI is sensitive to SCI in regions remote from injury, suggesting that the diffusion metrics may be used as a biomarker for severity of injury.

**Key words:** DTI; MRI; rat; SCI

## Introduction

MEASUREMENTS OF WATER DIFFUSION within the spinal cord after an injury, including measurements in regions distant from the injury site, may provide valuable insight into the severity of injury. Water diffusion within biological tissues can be measured noninvasively using magnetic resonance diffusion tensor imaging (DTI). As diffusion barriers within the tissue change after injury, DTI has provided researchers with an invaluable tool to monitor histological changes to the spinal cord after a spinal cord injury (SCI); however, most studies have focused on diffusion measurements at or within a few segments of the site of injury.<sup>1–3</sup> Although DTI at the injury site provides information about the histological structure of the injured spinal cord, imaging of the injury site after trauma in humans can be challenging. After injury, the spine tissues are disrupted, and stabilization devices are typically placed around the lesion site, which causes imaging artifacts in an MRI and prevents a physician from assessing the severity of an injury. The purpose of the current study was to determine whether DTI at sites rostral and caudal to the injury provided measures of injury severity in graded contusion injuries in rats.

DTI parameters of the spinal cord are sensitive to histological changes that occur after a traumatic injury. In addition to the primary injury, there is secondary damage to the spinal cord in regions

distant from the injury site that results in histological changes that affect water diffusion, including degeneration of fiber tracts, ischemia, edema, and oxidative damage to the tissue membranes that act as barriers to diffusion.<sup>4–6</sup> This inflammatory response results in impaired medullary circulation and changes to spinal cord structure, which consequently develops necrosis that has been documented throughout the entire length of the spinal cord, up to the brainstem.<sup>7</sup> The resulting demyelination of tracts at significant distances away from the lesion continues for >1 year.<sup>8</sup> These physical changes to the cellular microstructure, including axon number and volume changes, as well as alterations in intracellular and extracellular water balance, correlate with changes in apparent diffusion, including both longitudinal diffusion (along the tracts) and radial diffusion (across the spinal tracts).<sup>9</sup> Axon morphometric parameters in various white matter (WM) tracts appear to underlie differences in overall diffusion, which could be useful in detecting injury to spinal WM tracts.<sup>10</sup> Therefore, DTI measurements of diffusion throughout the spinal cord after an injury might be used as a biomarker for injury severity.

There is evidence of decreases in diffusivity of water in the spinal cord in regions rostral to a chronic injury, possibly as a result of secondary injury processes throughout the entire spinal cord. Previously, our group has found changes in diffusion of water along the entire length of the spinal cord after a moderate SCI to the

<sup>1</sup>Department of Biomedical Engineering, Marquette University, Milwaukee, Wisconsin.

<sup>2</sup>Department of Neurosurgery, Medical College of Wisconsin, Milwaukee, Wisconsin.

eighth thoracic vertebrae in rats.<sup>11</sup> Mean diffusivity (MD) significantly decreases in regions away from the lesion site, consistent with secondary injury processes such as cytotoxic edema, chronic atrophy, and axonal loss. Changes in MD have also been documented in the high cervical spinal cord (rostral to an injury) in humans with chronic SCI (cf. however, Petersen et al.).<sup>12–15</sup> These observations raise the question of whether changes in diffusivity in regions distant from the injury are related to injury severity. Further, it is expected that severity of injury changes the secondary injury processes, as the extent of demyelination and remyelination depend upon the number of axons that are disrupted by the injury.<sup>16</sup> The severity of injury also determines the time course of recovery; in cases of remyelination, smaller lesions acquire myelin sheath faster than larger ones.<sup>17</sup> Consequently, it might be possible to predict the severity of injury from diffusion measurements of the spinal cord over time. Recently, Kim et al. demonstrated that DTI of the injury site in the hyperacute stage (<3 h post-injury) can be used to predict functional recovery after a thoracic injury in rats.<sup>3</sup> Although promising, there is limited additional evidence that DTI of the injury site or elsewhere in the spinal cord correlates with functional recovery. In the current study we hypothesized that changes in DTI of the high cervical spinal cord are related to functional recovery in rats with low thoracic spinal contusions.

In order to determine whether MD varies with injury severity, we tested DTI in a contusion model of rat SCI using four different injury severities (control, mild, moderate, and severe). Rats were administered one of four severities of injury at the thoracic level (T8) and *ex vivo* DTI of the entire spinal cord was conducted at 10 weeks post-injury. Changes in diffusion characteristics of the cervical spinal cord were then correlated to behavioral tests of motor and sensory function. We hypothesized that there would be greater reduction in MD for specimens with more severe injuries.

## Methods

Forty female Sprague–Dawley rats (200–250 g) were used for this experiment. Rats were evenly divided into control, mild, moderate, and severe groups (i.e.,  $n = 10$  for each group) and given a contusion injury with the magnitude of the contusion severity determined by group categorization. Rats were then allowed to survive for 10 weeks, after which *ex vivo* DTI scans were performed on the spinal cord. All procedures were approved by the Institutional Animal Care and Use Committees (IACUC) at Marquette University, the Medical College of Wisconsin, and the Zablocki VA Medical Center.

### SCI procedure

A contusion injury was produced in each rat. Rats were first anesthetized with an intraperitoneal (IP) injection of 40  $\mu$ L xylazine, 0.1 mL of acepromazine, and 0.75  $\mu$ L of ketamine hydrochloride diluted 1:1 with deionized water. The initial dose of the anesthetic was 0.890 mL/kg of body weight, with additional anesthetic depending upon leg flexion-withdrawal and cornea reflexes. The rats were then shaved, sterilized with a povidone-iodine scrub pack, and secured to a surgical board. An incision was made over the mid-thoracic region, and a laminectomy was performed on the T7–T9 spinal segments. The rats were then placed in a MASCIS impactor (W.M. Keck Center for Collaborative Neuroscience; Piscataway, NJ) and a 10 g rod was dropped from a height of 0 mm, 10 mm, 25 mm, or 50 mm to induce a control, mild, moderate, or severe injury with kinetic energy immediately before impact equal to 0 J,  $9.80 \times 10^{-4}$  J,  $2.45 \times 10^{-3}$  J, and  $4.90 \times 10^{-3}$  J, respectively.

After surgery, rats were placed on postoperative care. The bi-daily procedure involved bladder expression, one dose of enro-

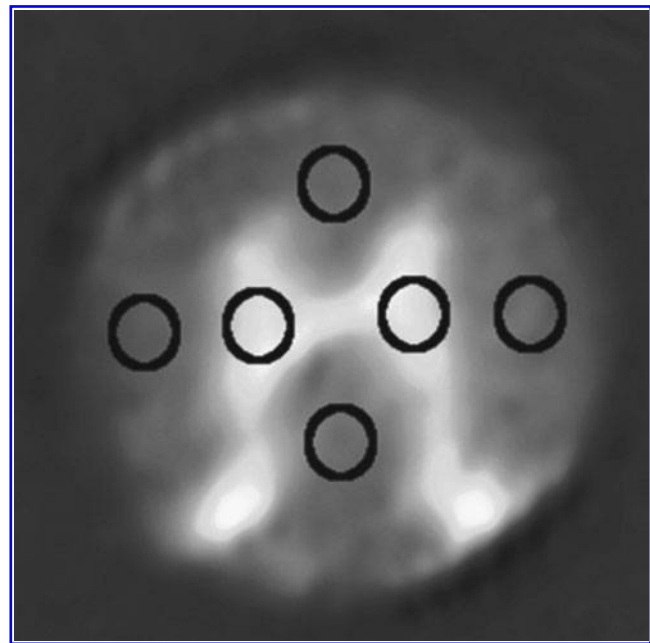


**FIG. 1.** Typical placement of individual region of interest drawings (ROIs) for dorsal, lateral, and ventral columns as well as gray matter. ROIs are overlaid onto a spin echo image.

floxacin (10 mg/kg subcutaneously; Bayer Healthcare LLC; Shawnee Mission, KS), buprenorphine hydrochloride (0.1–0.5 mg/kg subcutaneously; Rickitt Benckiser Health Care Ltd; Hull, UK), and 6 cc of lactated Ringer's solution. Animals were kept under postoperative care procedures until bladder function returned and specimens showed no signs of infection or stress. All rats survived the injury procedures and recovered in good health.

### Behavioral assessment

Open field walking was evaluated according to the Basso, Beattie, and Bresnahan (BBB) rating scale every week after the surgical procedure.<sup>18</sup> Following the standard BBB protocol, rats were placed on a flat, 1 M diameter surface and observed for 3 min. Hindlimb function was assessed according to the 0–21 BBB scoring, where 0 is flaccid paralysis and 21 is normal gait.

### Ex vivo MRI protocol

*Ex vivo* images were obtained at 11 weeks after injury. Animals were euthanized with an IP injection of sodium pentobarbital (100 mg/kg body weight) and perfused through the heart with a 300 mL saline buffer followed by 600 mL of 10% formalin. The spinal cords were extracted and post-fixed in a 10% formalin solution. On the day of the *ex vivo* scanning session, the spinal cords were embedded in an agarose gelatin mixture made of agarose powder dissolved in distilled H<sub>2</sub>O following the protocol of Ellingson et al.<sup>11</sup> Specimens were then placed in a 9.4T Bruker BioSpec 94/30 USR Spectroscopy Imaging System (Bruker BioSpin; Billerica, MA). A quadrature coil was used for transmitting and receiving radio signals (Doty Scientific; Columbia, SC). Diffusion weighted images (DWIs) were acquired using a six direction spin echo imaging sequence with a field of view (FOV) size of 5.12 cm, echo/repetition time of 31.6 ms/14 sec, 25 slices with a slice thickness of 2 mm, inter-slice gap of 1 mm, and number of excitations (NEX) of two so that our scan sessions were roughly 13 h per scan. Our rationale for the 2 mm slice thickness was that it provided an adequate signal-to-noise ratio (SNR) and adequate

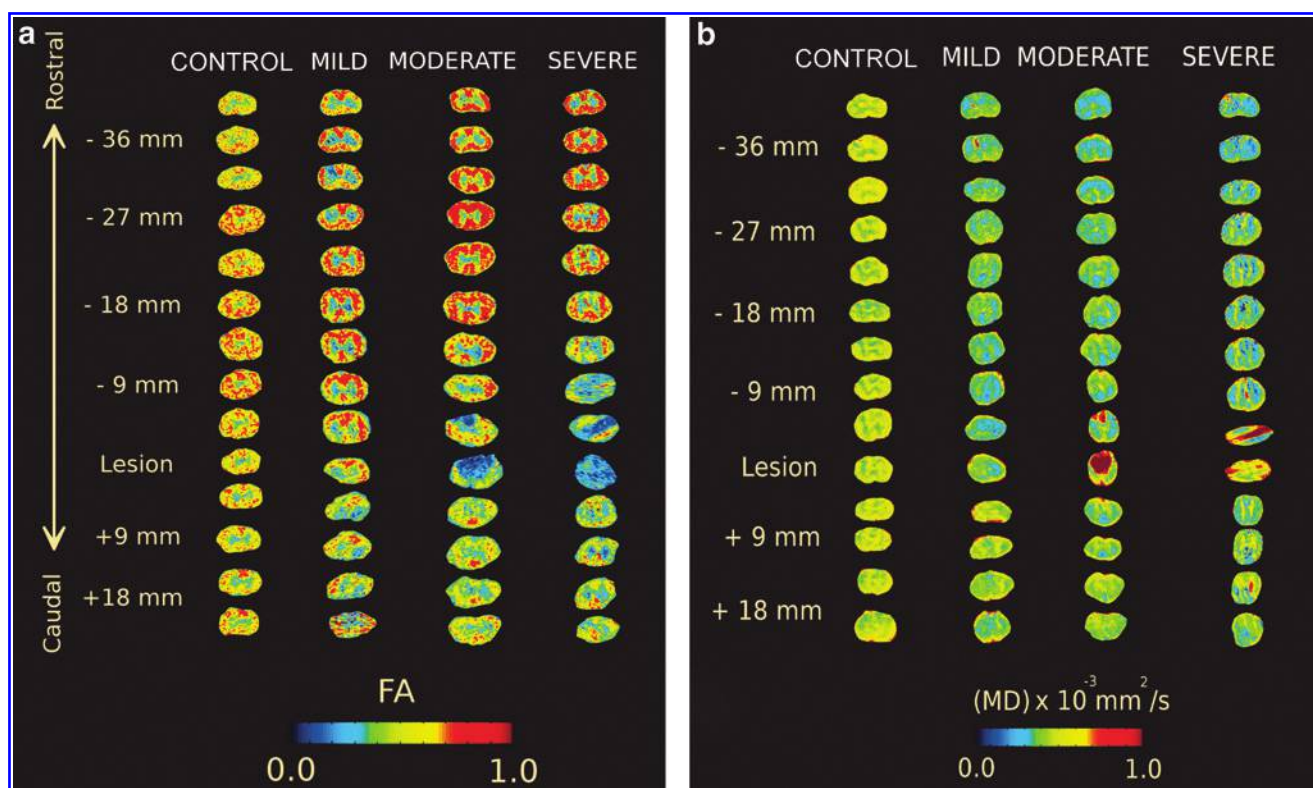


**FIG. 2.** Regions of interest (ROIs) taken for fractional anisotropy (FA) (a) and mean diffusivity (MD) (b) over the entire length of the cord. One rat was randomly selected from each group and the ROIs were extracted for the entire length of the cord. Separation between white and gray matter was disrupted severely around injury sites for both FA and MD. Color-coded intensity values change as severity of injury is increased across spinal segments.

resolution for this analysis and facilitated scanning in the desired scan time. The matrix size was  $512 \times 512$ , and the b-values were 0 and  $500 \text{ s/mm}^2$ . A b-value of  $500 \text{ s/mm}^2$  was chosen to image the fast diffusion compartments and provide a relatively high SNR, similar to the study by Ellingson et al.<sup>11</sup>

#### DTI analysis

DTI parameters were then calculated for the entire sample. Images were imported into the Analysis of Functional NeuroImages software package (AFNI; available at <http://afni.nimh.nih.gov/>). The DWIs were then co-registered to the b0 images, using an iterative weighted least squares fit to the T2-weighted images to correct for eddy current and susceptibility distortions. Following registration, the resulting matrix volume data were used to calculate the DTIs from the DWIs. The eigenvalues ( $\lambda_1$ ,  $\lambda_2$ ,  $\lambda_3$ ) and vectors were calculated from the  $3 \times 3$  diffusion tensor. The eigenvalues were then used to calculate diffusion indices. The indices included the longitudinal diffusion coefficient (LD), represented by  $\lambda_1$ , and the radial diffusion coefficient (RD) calculated by the mean of eigenvalues  $\lambda_2$  and  $\lambda_3$ . The MD was also calculated as the trace of the tensor (i.e., the mean of all three eigenvalues). The fractional anisotropy (FA), which represents the overall anisotropy of diffusion at a certain voxel, was calculated using the formula prescribed by Basser et al.<sup>19</sup>

Image analysis was then completed in Matlab (The MathWorks Inc; Natick, MA). Regions of interests (ROIs) were manually found for each of the diffusion indices in each axial slice. One ROI was defined as the entire transverse cord (i.e., the whole cord ROI). Separate ROIs were also identified for gray matter (GM), as well as dorsal columns (DWM), lateral columns (LWM), and ventral columns (VWM) in the WM segments, as shown in Figure 1. The average diffusion indices for the LWM and GM ROIs were found

by combining the left and right ROIs. The entire data set for a rat was excluded if significant variations in image quality were found as a result of image ghosting, low SNR ( $> 2$  SD of average group SNR), or if the specimen produced an outlier during BBB scoring that was not consistent with severity level (i.e., severe injuries were

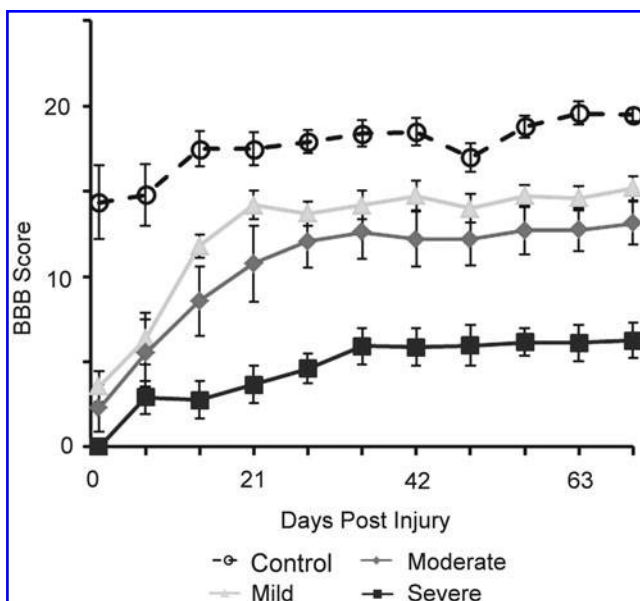


**FIG. 3.** Basso, Beattie, and Bresnahan (BBB) score depicting rat recovery following spinal cord injury for each severity over 10 weeks. Error bars indicate the standard deviation.



TABLE 1. DTI METRICS FOR CONTROL SPINAL CORDS

	FA	MD ( $\times 10^{-3}$ mm <sup>2</sup> /sec)	LADC ( $\times 10^{-3}$ mm <sup>2</sup> /sec)	TADC ( $\times 10^{-3}$ mm <sup>2</sup> /sec)
Whole cord	0.51 $\pm$ 0.003	0.75 $\pm$ 0.004	1.01 $\pm$ 0.012	0.56 $\pm$ 0.013
White matter	0.58 $\pm$ 0.060	0.71 $\pm$ 0.048	0.93 $\pm$ 0.003	0.45 $\pm$ 0.049
Gray matter	0.31 $\pm$ 0.095	0.78 $\pm$ 0.052	0.71 $\pm$ 0.104	0.68 $\pm$ 0.052

The mean and standard deviation for DTI metrics in different ROIs.

DTI, diffusion tensor imaging; FA, fractional anisotropy; MD, mean diffusivity; LADC, isotropic apparent diffusion coefficient; TADC, transverse apparent diffusion coefficient; ROI, region of interest.

expected to have a BBB score  $< 7$  on both limbs at 10 weeks following an injury, and control injuries were expected to have a BBB score  $> 18$  on both limbs at 10 weeks following an injury). The resulting groups were as follows, control ( $n=8$ ), severe ( $n=8$ ), moderate ( $n=9$ ), and mild ( $n=10$ ).

### Statistical analysis

All statistical analyses were conducted using the Statistical Package for Social Sciences (SPSS version 13.0; SPSS Inc., Chicago, IL). A Student's *t* test was performed to determine statistical significance between the DTI indices of the SCI rats and controls on a slice-by-slice basis as well as an average of the overall DTI index in the cervical or thoracic region. Each ROI was averaged at each slice location across all specimens. A two way, repeated measures, analysis of variance (ANOVA) (fixed factors: injury group and slice location [C1-T10 with roughly two slices per segment]; random factor: specimen) was also completed to look at variations across groups.  $P < 0.05$  was considered to be statistically significant. A Tukey post-hoc test for multiple comparisons was also performed to compare between spinal levels. The correlation between injury group and BBB score was analyzed using the Spearman correlation.

### Results

Images of FA and MD in axial slices of the spinal cord are shown in Figure 2 for representative specimens from each severity group. A distinction between white and GM regions was observed in all specimens, especially for FA images. Near the injury site in moderately and severely injured rats, the GM and WM tracts were harder to distinguish visually. In addition, the MD appeared to be lower in more severely injured specimens, and this lower diffusivity was observed throughout the volume of the spinal cord, except near the lesion. This separation was consistent with the BBB functional motor tests at week 10, which corresponded to the *ex vivo* scan time points. Interestingly, there was no significance ( $p > 0.05$ ) in the BBB scores at week 10, for mildly and moderately injured rats, as seen in Figure 3.

#### DTI indices in the control group

DTI indices were consistent over the length of the spinal cord for the control group. Mean ROIs within the control group, for FA, MD, LD, and RD, had low within-group variations for each DTI index (mean and SD for the DTI indices are given in Table 1). The variation was smaller for the analysis of the whole cord ROI, with the maximum coefficient of variation (CoV) occurring in RD (2.32%). The WM and GM regions were slightly more variable, with the largest CoV equal to 14.65% in the GM LD. Overall, SD was low for each group, demonstrating consistency within the MRI scanning. As shown in Table 1, the average FA in WM was greater than the whole cord and GM ROIs; conversely, MD, LD, and RD for WM were considerably lower than the whole cord values, but

within each WM/GM ROI, these DTI parameters were still consistent over the length of the cord.

#### Whole cord ROI analysis

There was a strong correlation between mean MD across the spinal cord and BBB score ( $r^2=0.80$ ), as seen in Figure 4. Mean FA, MD, LD, and RD were calculated for each specimen, over the C1-C7 cervical segments for each specimen, and compared with individual BBB scores. The resulting correlations ranged from  $r=0.53$  to  $0.94$  in WM ROIs, and between  $r=0.33$  and  $0.82$  in the GM ROI, as shown in Table 2. The stronger correlations ( $r > 0.7$ ) occurred in MD, LD, and RD. All groups had a significance of  $p < 0.001$  with the exception of LD for LWM and FA for GM, which were significant at the  $p < 0.01$  level.

There was variation in DTI indices along the length of the spinal cord, with notable differences at the injury site. DTI indices for each slice were analyzed from  $-40$  mm rostral to the injury site to  $20$  mm caudal to the injury site as shown in Figure 5. Visually, there was a clear separation among severity groups throughout the entire length of the cord, with the greatest difference occurring in mean diffusivity, which showed an 18% reduction for regions cephalad to injury. This separation is also represented in Figure 6 with mild, moderate, and severe groups being significantly different than the control group when comparing average MD across the C1-C7 cervical segments for each specimen. Comparing GM and WM tracts (Fig. 7), the separation among groups was consistent over the length

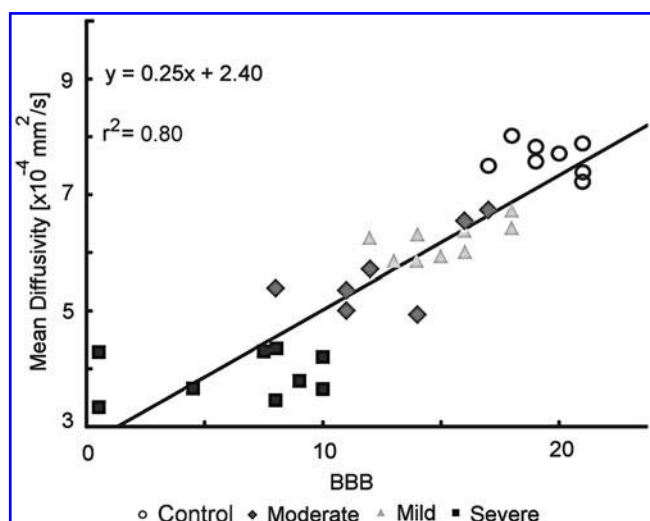


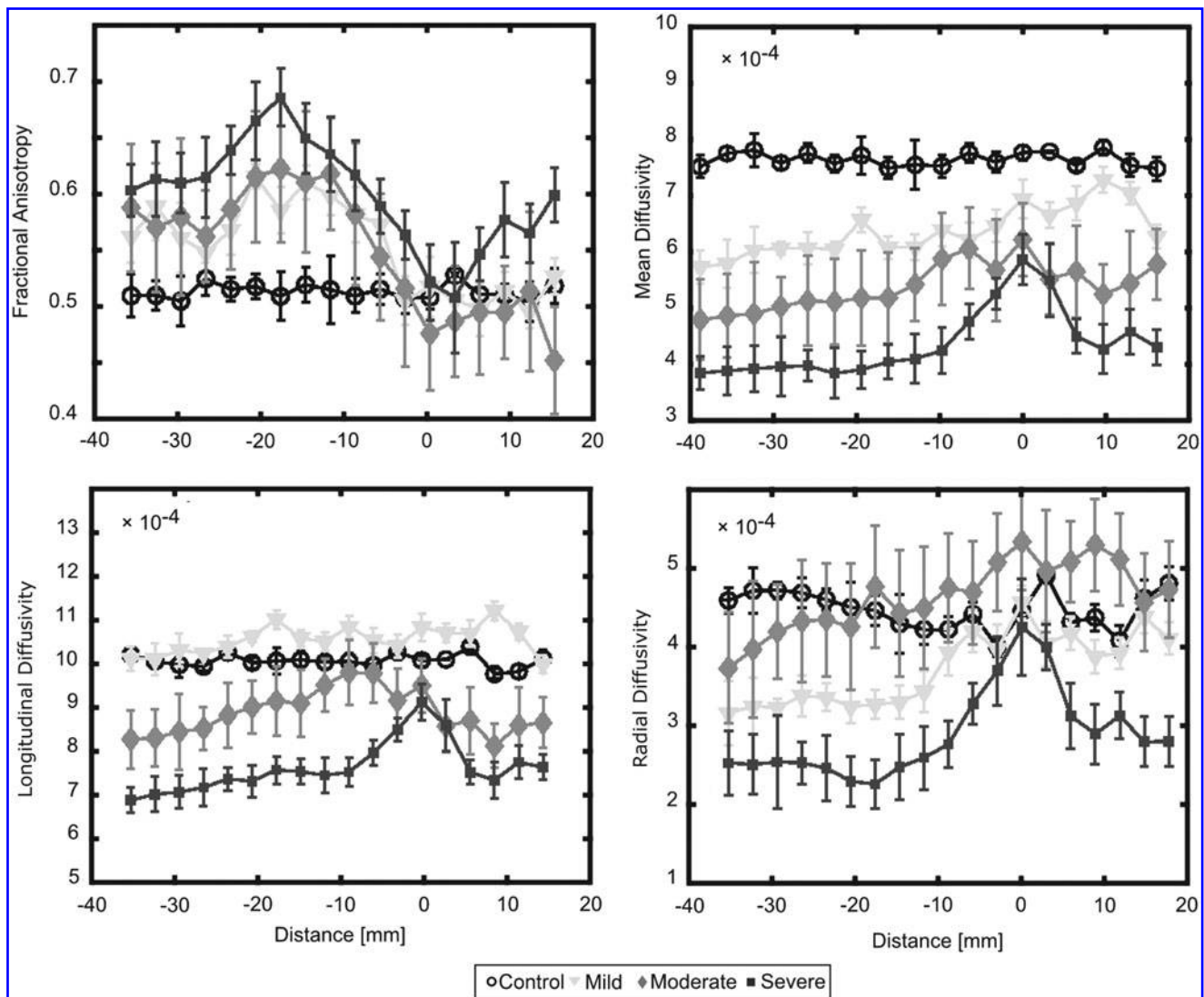
FIG. 4. Whole cord mean diffusivity (MD), averaged across slices, correlated to individual Basso, Beattie, and Bresnahan (BBB) scores. An  $r^2=0.80$  demonstrates a strong correlation between MD of the cervical spinal cord compared with average BBB score of rats at week 10.

TABLE 2. BBB SCORE CORRELATION WITH WHOLE CORD ROI FOR DTI METRICS

	FA	MD	LADC	TADC
Whole Cord	-0.548 (<0.001)	0.935 (<0.001)	0.785 (<0.001)	0.868 (<0.001)
VWM	0.609 (<0.001)	0.759 (<0.001)	0.700 (<0.001)	0.575 (<0.001)
DWM	0.575 (<0.001)	0.829 (<0.001)	0.681 (<0.001)	0.565 (<0.001)
LWM	0.565 (<0.001)	0.752 (<0.001)	0.527 (0.001)	0.899 (<0.001)
GM	0.329 (0.006)	0.783 (<0.001)	0.531 (<0.001)	0.818 (<0.001)

Spearman correlation coefficients ( $p$  values in parentheses) for the correlation between BBB scores for individual rats and their ROIs across the individual DTI metrics (FA, MD, LADC, and TADC).

BBB, Basso, Beattie, and Bresnahan; ROI, region of interest; DTI, diffusion tensor imaging; FA, fractional anisotropy; MD, mean diffusivity; LADC, isotropic apparent diffusion coefficient; TADC, transverse apparent diffusion coefficient; VWM, ventral columns in white matter; DWM, dorsal columns in white matter; LWM, lateral columns in white matter; GM, gray matter.



**FIG. 5.** A comparison between severity groups rostral and caudal to the injury site. Here the injury site is located at 10 mm. Fractional anisotropy (FA), mean diffusivity (MD), longitudinal diffusion coefficient (LD), and radial diffusion coefficient (RD) are shown for a whole cord region of interest (ROI) that includes white and gray matter. Spinal cord regions at and around the lesion site (0 mm) demonstrated drastically altered diffusion values compared with distal regions of the spinal cord. The clearest separation of diffusion values for each of the severity groups was observed in the mean diffusivity metric. Error bars indicate the standard deviation.

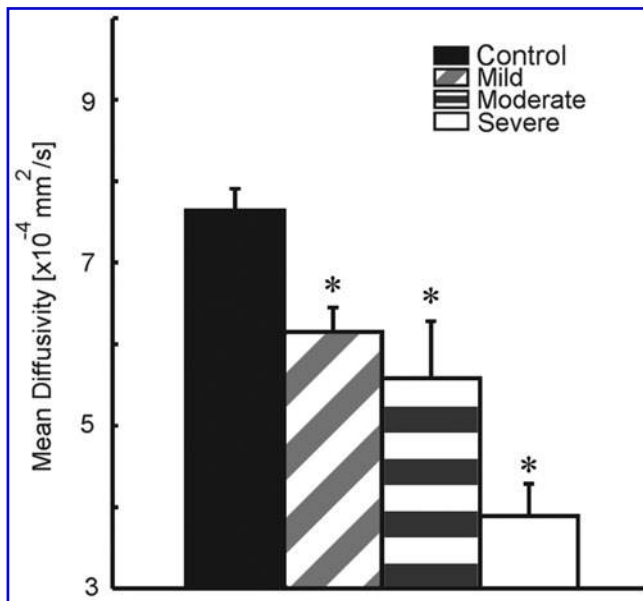


**FIG. 6.** Average mean diffusivity (MD) over the cervical segments of the spinal cord for each severity group. Mild, moderate, and severe injuries were significantly different than the control group (\* $p < 0.05$ ). Error bars indicate the standard deviation for each group.

of the cord for WM tracts. The GM also showed separation based on severity, which was most visually apparent in MD and RD.

Statistical differences were found among severity groups for the DTI indices and ROIs, with some exceptions. In comparing the different severity groups over the entire length of the cord (Table 3), VWM, DWM, LWM, and GM were statistically different ( $p < 0.01$ ) between the severe injury group and the other groups in all indices except when compared with moderate injuries for FA and MD in VWM, DWM, LWM, and GM. LD and RD showed significant differences ( $p < 0.01$ ) among groups in all of the ROIs except between the mild and control groups in VWM, and the mild and moderate groups in VWM and DWM for LD only. Conversely, the control and mildly injured rats were not significantly different for any of the DTI metrics ( $p > 0.05$ ). There was also no significant difference ( $p > 0.05$ ) between RD values at, and caudal to, the site of injury. In addition, no significant difference ( $p > 0.05$ ) was observed for FA in GM between the mild and severe injuries. Other comparisons between groups showed that FA was not significantly different between the control group and the mild group for any ROIs or for the control group and the moderate group in VWM, DWM, LWM, and GM.

## Discussion

Results from this study suggest that DTI is sufficiently sensitive to detecting secondary injury rostral to a contusion injury site. These secondary injury effects were manifested as a decrease in mean diffusivity in the cervical spinal cord following a thoracic (T8) contusion that was proportional to the severity of injury. We observed a strong correlation ( $r^2 = 0.80$ ) between MD of the cervical spinal cord and functional outcome, measured by the BBB motor score. Changes in diffusivity were also noted at the primary injury site, with relative changes along the length of the spinal cord that were consistent with reported results at or near the injury.<sup>1,11,20</sup>

The decreases in MD as well as the changes in FA may appear counterintuitive to previous literature that has focused on the injury site.<sup>1,11,20</sup> Our results demonstrated an increase in MD at the injury site compared with the rest of the cord, similar to those previous studies; however, in remote regions, MD is decreased. The new findings verify the decrease in MD found in rodents and humans following an SCI.<sup>12,14</sup> We believe the counterintuitive nature of the changes in diffusivity remote from the region site could be reflective of changes in axon and myelin structure, intracellular and extracellular water balance, and edema or inflammatory processes.

### *Diffusivity measures reflect documented histological changes in the spinal cord*

Variations in diffusivity measures away from the injury site likely reflect changes in tissue structure. Our results include a clear decrease in mean diffusivity following SCI at regions distal to the injury. These results support similar data from Takahashi et al., who reported a decrease in diffusion in regions remote from the site of injury during the degeneration and regeneration of sea lamprey axons.<sup>21</sup> The decrease in diffusivity in our results could reflect membrane structural changes associated with myelin and axonal degeneration. We observed decreases in both RD and LD in the cervical spinal cord in the current study. Changes in RD have been associated with cell membrane and myelin sheath permeability to water, although RD has been shown to not be strongly correlated with myelin sheath thickness.<sup>22,23</sup> Conversely, LD decreases with decreased myelin thickness and smaller axon diameter, and LD is associated with neurofilament and microtubule density.<sup>3,9,22,24</sup> The LD and RD metrics do not always change in parallel; LD has been shown to change when RD does not, suggestive of axonal degeneration and not myelin degeneration.<sup>25</sup> Therefore, the decreases in both longitudinal and radial diffusivity observed in the current study could be associated with changes in axon and myelin structure that accompany Wallerian degeneration.

Extra-axonal tissue changes could also have affected the diffusivity measurements in WM tracts. The decrease in diffusivity that we observed was correlated with the severity for up to 40 mm rostral to the injury site, which is consistent with a cellular reaction. Wallerian degeneration in the cervical dorsal columns from a thoracic injury results in microglial and astroglial reactions, with an eventual astroglial scar.<sup>4,15,26–28</sup> This cell proliferation and scar formation would be expected to decrease diffusivity in all directions, consistent with our observations. In addition to the cell and scar tissue itself, changes in extracellular matrix proteoglycans, which are increased after central nervous system (CNS) injury, could also affect water diffusion.<sup>29</sup> Scarring and other changes in the extracellular matrix likely account for the decreased diffusivity of the cervical spinal cord after thoracic injury that was observed in the current study; however, the influx of a cellular response to injury may also play a role.

The change in diffusion barriers associated with tissue breakdown and influx of inflammatory cells as time progresses could also explain the decline in diffusivity that we observed away from the injury site. Following cortical impact and the resulting axonal damage, there is a decrease in MD and an increase in FA suggestive of cytotoxic edema.<sup>30</sup> Changes in tissue structure in regions outside the lesion site attributed to cytotoxic inflammatory products were implicated in this brain study.<sup>30</sup> In general, there is strong evidence of changes in the number of inflammatory cells at locations away from the injury site and even outside of the spinal cord.<sup>31–35</sup> The activation of the inflammatory processes helps to explain the

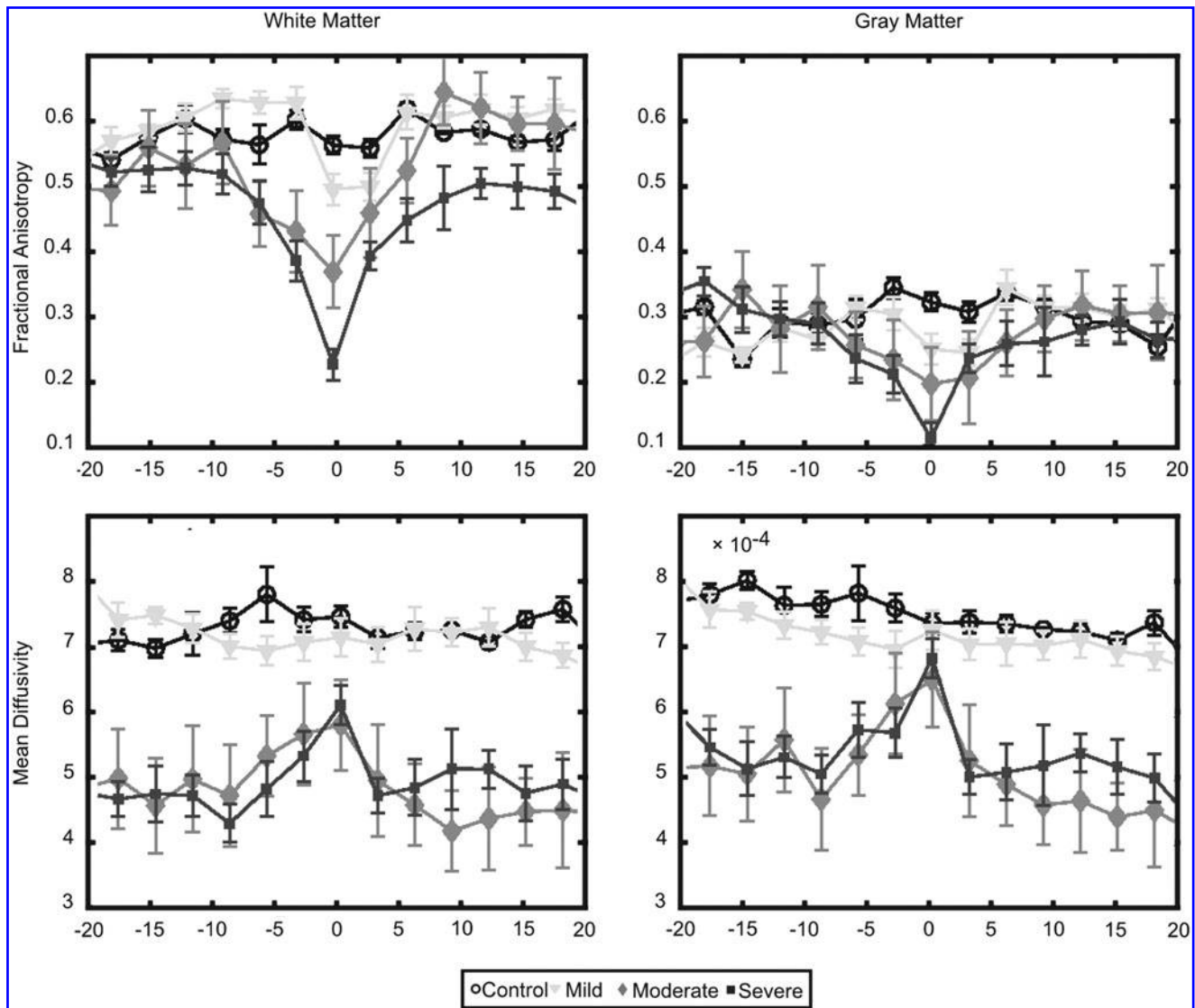


**FIG. 7.** A comparison between white and gray matter values for fractional anisotropy (FA) and mean diffusivity (MD). The comparison extended over 20 mm rostral and caudal to the injury site (0 mm). Drastic difference in white and gray matter values are shown, with the most severe changes in diffusion occurring around the lesion site. FA and MD were sensitive to diffusion changes at the lesion site for white matter. FA was less altered in gray matter at the lesion site when comparing groups. Error bars indicate the standard deviation.

changes in water diffusion following SCI in regions remote from the injury site, although changes in water balance between intracellular and extracellular compartments cannot be excluded.

#### *Diffusivity and changes in water balance*

Results from this study are also consistent with the concept that DTI is sensitive to changes in intracellular and extracellular water compartments. The decrease in water diffusion that we observed following injury has also been reported following injury to the CNS.<sup>36–38</sup> It has been proposed that the primary reason for this decrease is the relationship between the intra- and extracellular water compartments, specifically, the resulting decrease in intracellular water diffusion.<sup>39</sup> In cerebral ischemia, the intracellular water compartment is the overall determinant of changes in water diffusion.<sup>40</sup> These studies raise the possibility that ischemia within the spinal cord after an injury might underlie the reduction in apparent diffusion coefficient (ADC).

In addition, the observed changes in diffusivity that we saw might have been reflected by a change in water balance caused by edema or other inflammatory processes. Upregulation of the primary water channel, aquaporin-4, has been reported in areas away from the lesion site in chronic injury, suggesting altered water transport, edema, and syringomyelia.<sup>41</sup> Changes in water balance are thought to greatly affect the diffusion of water within tissue.<sup>2,11,42</sup> The significant decrease in the diffusion values for MD, LD, and RD appear to suggest that the changes to the cellular fluidic environment could be a direct cause of the changes to water diffusion; however, further investigation into the water volume shift between intracellular and extracellular compartments is needed.

#### *Diffusivity in GM*

Changes in GM diffusivity in the current study suggest that the decreased diffusivity of the cervical spinal cord cannot be entirely attributed to changes in structure of the WM tracts associated with



TABLE 3. ANALYSIS OF DIFFERENCES AMONG GROUPS

WC	FA			MD		
	Mild	Moderate	Severe	Mild	Moderate	Severe
Control	0.274	0.233	<0.001	<0.001	<0.001	<0.001
Mild	-	1.000	0.001	-	<0.001	<0.001
Moderate		-	0.001		-	<0.001
	LD			RD		
	Mild	Moderate	Severe	Mild	Moderate	Severe
Control	0.004	<0.001	<0.001	<0.001	<0.001	<0.001
Mild	-	<0.001	<0.001	-	0.039	<0.001
Moderate		-	<0.001		-	<0.001
VWM	FA			MD		
	Mild	Moderate	Severe	Mild	Moderate	Severe
Control	0.977	0.017	<0.001	0.039	<0.001	<0.001
Mild	-	0.050	<0.001	-	<0.001	<0.001
Moderate		-	0.065		-	0.061
	LD			RD		
	Mild	Moderate	Severe	Mild	Moderate	Severe
Control	0.760	0.001	<0.001	0.914	<0.001	<0.001
Mild	-	0.016	<0.001	-	<0.001	<0.001
Moderate		-	<0.001		-	<0.001
DWM	FA			MD		
	Mild	Moderate	Severe	Mild	Moderate	Severe
Control	0.516	0.182	<0.001	<0.001	<0.001	<0.001
Mild	-	0.006	<0.001	-	<0.001	<0.001
Moderate		-	0.014		-	0.707
	LD			RD		
	Mild	Moderate	Severe	Mild	Moderate	Severe
Control	0.728	0.004	<0.001	<0.001	<0.001	<0.001
Mild	-	0.066	<0.001	-	<0.001	<0.001
Moderate		-	0.001		-	<0.001
LWM	FA			MD		
	Mild	Moderate	Severe	Mild	Moderate	Severe
Control	0.842	0.144	<0.001	0.989	<0.001	<0.001
Mild	-	0.020	<0.001	-	<0.001	<0.001
Moderate		-	0.074		-	0.052
	LD			RD		
	Mild	Moderate	Severe	Mild	Moderate	Severe
Control	0.647	0.441	<0.001	0.001	<0.001	<0.001
Mild	-	0.046	<0.001	-	<0.001	<0.001
Moderate		-	<0.001		-	<0.001
GM	FA			MD		
	Mild	Moderate	Severe	Mild	Moderate	Severe
Control	0.325	0.148	0.015	0.136	<0.001	<0.001
Mild	-	0.972	0.515	-	<0.001	<0.001
Moderate		-	0.781		-	0.064
	LD			RD		
	Mild	Moderate	Severe	Mild	Moderate	Severe
Control	0.308	0.807	<0.001	0.084	<0.001	<0.001
Mild	-	0.829	<0.001	-	<0.001	<0.001
Moderate		-	<0.001		-	<0.001

The differences among group means for each severity group are shown above. *P* values from analysis of variance (ANOVA) results for the differences between each of the severity groups for each diffusion tensor imaging (DTI) metric are shown for whole cord (WC), ventral white matter (VWM), dorsal white matter (DWM), lateral white matter (LWM), over all white matter (WM) and overall gray matter (GM) region of interest drawings (ROIs). Comparisons were made for the fractional anisotropy (FA), mean diffusivity (MD), longitudinal diffusivity (LD), and the radial diffusivity (RD) diffusion metrics.

Wallerian degeneration. The diffusivity changes in cervical GM and WM were very similar. Whereas changes in diffusivity related to Wallerian degeneration has been a focus of DTI studies after injury, GM diffusion changes suggest that the entire spinal cord is involved.<sup>23,43–45</sup> A limited number of studies have reported diffusion characteristics from GM regions, and it is thought that some of these changes occur because of astrocytic activity in GM triggered by Wallerian degeneration in WM.<sup>28,38,46</sup> The similarity of changes in diffusion of both GM and WM is also consistent with a generalized change in water balance throughout the spinal cord.

### Study limitations

Changes in MD were consistently observed in the GM and individual tract ROIs, although the statistical tests were less conclusive than the whole cord ROI. The increased variability caused by the smaller size of the individual tract ROIs most likely accounted for the differences in the statistical tests. There has been a persistent interest in imaging specific tracts of the spinal cord following an injury in order to ascertain whether functional outcomes might be associated with particular tract loss.<sup>2,3,12</sup> As such, there has been a desire to obtain improved resolution images with higher SNR.<sup>47–49</sup> The current study benefited in this regard from the use of *ex vivo* scans; however, additional resolution and improved SNR might be obtained with new coil designs and improved image sequences. Although image quality is important, especially with the use of the lower quality *in vivo* scans, the current results suggest that a whole cord ROI provides reasonable estimates of useful DTI metrics. As similar changes occur throughout GM and WM, a whole cord ROI, for which it is relatively easy to delineate between cord and the surrounding cerebrospinal fluid, might be the best option for identifying a DTI parameter that reflects injury severity.

The primary and secondary damage resulting after an SCI are complex events occurring throughout the spinal cord. Although there are several hypotheses to account for changes in spinal cord tissue diffusivity away from the injury site, a more accurate assessment using histological and immunohistochemical techniques is needed. Staining for neurofilament density with SMI-31 and SMI-32 for example, has been associated with changes to water diffusion.<sup>3,24</sup> Measurements of astrocyte and macrophage interactions in the cervical segments of the spinal cord might offer better insight into the severity-related changes that are picked up by diffusion measurements. Examining the degradation of glial fibrillary acidic protein (GFAP) to assess the axonal degradation along the cord may also be a promising avenue of future research.

### Conclusion

In conclusion, we have demonstrated that diffusivity in the spinal cord rostral to the injury site varies with injury severity, and that *ex vivo* DTI is sufficiently sensitive to these changes. Therefore, rostral DTI may be a valuable biomarker for varying injury severity in more caudal levels of the spinal cord. Our results support the hypothesis that injury severity is associated with respective diffusion changes over the entire length of the spinal cord.

### Acknowledgments

This material is based on work supported by the Department of Veterans Affairs.

### Author Disclosure Statement

No competing financial interests exist.

### References

- Deo, A., Grill, R., Hasan, K., and Narayana, P. (2006). In vivo serial diffusion tensor imaging of experimental spinal cord injury. *J. Neurosci. Res.* 83, 801–810.
- Sundberg, L., Herrera, J., and Narayana, P. (2010). In vivo longitudinal MRI and behavioral studies in experimental spinal cord injury. *J. Neurotrauma* 27, 1753–1767.
- Kim, J., Song, S., Burke, D., and Magnuson, D. (2012). Comprehensive locomotor outcomes correlate to hyperacute diffusion tensor measures after spinal cord injury in the adult rat. *Exp. Neurol.* 235, 188–196.
- Avellino, A., Hart, D., Dailey, A., MacKinnon, M., Ellegala, D., and Klot, M. (1995). Differential macrophage responses in the peripheral and central nervous system during wallerian degeneration of axons. *Exp. Neurol.* 136, 183–198.
- Carlson, S., Parrish, M., Springer, J., Doty, K., and Dossett, L. (1998). Acute inflammatory response in spinal cord following impact injury. *Exp. Neurol.* 151, 77–88.
- Kakulas, B. (2004). Neuropathology: the foundation for new treatments in spinal cord injury. *Spinal Cord* 42, 549–563.
- Ito, T., Oyanagi, K., Wakabayashi, K., and Ikuta, F. (1996). Traumatic spinal cord injury: a neuropathological study on the longitudinal spreading of the lesions. *Acta Neuropathol.* 93, 13–18.
- Totoiu, M., and Keirstead, H. (2005). Spinal cord injury is accompanied by chronic progressive demyelination. *J. Comp. Neurol.* 486, 373–383.
- Schwartz, E., and Hackney, D. (2003). Diffusion-weighted MRI and the evaluation of spinal cord axonal integrity following injury and treatment. *Exp. Neurol.* 184, 570–589.
- Gullapalli, J., Krejza, J., and Schwartz, E. (2006). In vivo DTI evaluation of white matter tracts in rat spinal cord. *J. Magn. Reson. Imaging* 24, 231–234.
- Ellingson, B., Kurpad, S., and Schmit, B. (2008). Ex vivo diffusion tensor imaging and quantitative tractography of the rat spinal cord during long-term recovery from moderate spinal contusion. *J. Magn. Reson. Imaging* 28, 1068–1079.
- Ellingson, B., Kurpad, S., and Schmit, B. (2008). Functional correlates of diffusion tensor imaging in spinal cord injury. *Biomed. Sci. Instrum.* 44, 28–33.
- Ellingson, B., Ulmer, J., Kurpad, S., and Schmit, B. (2008). Diffusion tensor MR imaging in chronic spinal cord injury. *AJNR Am. J. Neuroradiol.* 29, 1976–1982.
- Cheran, S., Shanmuganathan, K., Zhuo, J., Mirvis, S., Araabi, B., Alexander, M., and Gullapalli, R. (2011). Correlation of MR diffusion tensor imaging parameters with ASIA motor scores in hemorrhagic and nonhemorrhagic acute spinal cord injury. *J. Neurotrauma* 28, 1881–1892.
- Petersen, J., Wilm, B., von Meyenburg, J., Schubert, M., Seifert, B., Najafi, Y., Dietz, V., and Kollias, S. (2012). Chronic cervical spinal cord injury: DTI correlates with clinical and electrophysiological measures. *J. Neurotrauma* 29, 1556–1566.
- Schwab, M., and Bartholdi, D. (1996). Degeneration and regeneration of axons in the lesioned spinal cord. *Physiol. Rev.* 76, 319–370.
- Harrison, B., and McDonald, W. (1977). Remyelination after transient experimental compression of the spinal cord. *Ann. Neurol.* 1, 542–551.
- Basso, D., Beattie, M., and Bresnahan, J. (1995). A sensitive and reliable locomotor rating scale for open field testing in rats. *J. Neurotrauma* 12, 1–21.
- Basser, P., and Pierpaoli, C. (1996). Microstructural and physiological features of tissues elucidated by quantitative-diffusion-tensor MRI. *J. Magn. Reson. B.* 111, 209–219.
- Nevo, U., Hauben, E., Yoles, E., Agranov, E., Akselrod, S., Schwartz, M., and Neeman, M. (2001). Diffusion anisotropy MRI for quantitative assessment of recovery in injured rat spinal cord. *Magn. Reson. Med.* 45, 1–9.
- Takahashi, M., Hackney, D., Zhang, G., Wehrli, S., Wright, A., O'Brien, W., Uematsu, H., Wehrli, F., and Selzer, M. (2002). Magnetic resonance microimaging of intraaxonal water diffusion in live excised lamprey spinal cord. *Proc. Natl. Acad. Sci. U. S. A.* 99, 16,192–16,196.
- Schwartz, E., Cooper, E., Fan, Y., Jawad, A., Chin, C., Nissanov, J., and Hackney, D. (2005). MRI diffusion coefficients in spinal cord correlate with axon morphometry. *Neuroreport* 16, 73–76.

23. Kozłowski, P., Raj, D., Liu, J., Lam, C., Yung, A., and Tetzlaff, W. (2008). Characterizing white matter damage in rat spinal cord with quantitative MRI and histology. *J. Neurotrauma* 25, 653–676.
24. DeBoy, C., Zhang, J., Dike, S., Shats, I., Jones, M., Reich, D., Mori, S., Nguyen, T., Rothstein, B., Miller, R., Griffin, J., Kerr, D., and Calabresi, P. (2007). High resolution diffusion tensor imaging of axonal damage in focal inflammatory and demyelinating lesions in rat spinal cord. *Brain* 130, 2199–2210.
25. Konomi, T., Fujiyoshi, K., Hikishima, K., Komaki, Y., Tsuji, O., Okano, H., Toyama, Y., Okano, H., and Nakamura, M. (2012). Conditions for quantitative evaluation of injured spinal cord by in vivo diffusion tensor imaging and tractography: Preclinical longitudinal study in common marmosets. *Neuroimage* 63, 1841–1853.
26. Buss, A., and Schwab, M. (2003). Sequential loss of myelin proteins during Wallerian degeneration in the rat spinal cord. *Glia* 42, 424–432.
27. Griffin, J., George, R., Lobato, C., Tyor, W., Yan, L., and Glass, J. (1992). Macrophage responses and myelin clearance during Wallerian degeneration: relevance to immune-mediated demyelination. *J. Neuroimmunol.* 40, 153–165.
28. Buss, A., Brook, G., Kakulas, B., Martin, D., Franzen, R., Schoenen, J., Noth, J., and Schmitt, A. (2004). Gradual loss of myelin and formation of an astrocytic scar during Wallerian degeneration in the human spinal cord. *Brain* 127, 34–44.
29. Vorisek, I., Hájek, M., Tintera, J., Nicolay, K., and Syková, E. (2002). Water ADC, extracellular space volume, and tortuosity in the rat cortex after traumatic injury. *Magn. Reson. Med.* 48, 994–1003.
30. Xu, S., Zhuo, J., Racz, J., Shi, D., Roys, S., Fiskum, G., and Gullapalli, R. (2011). Early microstructural and metabolic changes following controlled cortical impact injury in rat: a magnetic resonance imaging and spectroscopy study. *J. Neurotrauma* 28, 2091–2102.
31. Koshinaga, M., and Whittemore, S. (1995). The temporal and spatial activation of microglia in fiber tracts undergoing anterograde and retrograde degeneration following spinal cord lesion. *J. Neurotrauma* 12, 209–222.
32. Moisse, K., Welch, I., Hill, T., Volkening, K., and Strong, M. (2008). Transient middle cerebral artery occlusion induces microglial priming in the lumbar spinal cord: a novel model of neuroinflammation. *J. Neuroinflammation* 5, 29–38.
33. Shi, F., Zhu, H., Yang, S., Liu, Y., Feng, Y., Shi, J., Xu, D., Wu, W., You, S., Ma, Z., Zou, J., Lu, P., and Xu, X. (2009). Glial response and myelin clearance in areas of wallerian degeneration after spinal cord hemisection in the monkey *Macaca fascicularis*. *J. Neurotrauma* 26, 2083–2096.
34. Weishaupt, N., Silasi, G., Colbourne, F., and Fouad, K. (2010). Secondary damage in the spinal cord after motor cortex injury in rats. *J. Neurotrauma* 27, 1387–1397.
35. Gris, D., Hamilton, E., and Weaver, L. (2008). The systemic inflammatory response after spinal cord injury damages lungs and kidneys. *Exp. Neurol.* 211, 259–270.
36. Moseley, M., Cohen, Y., Kucharczyk, J., Mintorovitch, J., Asgari, H., Wendland, M., Tsuruda, J., and Norman, D. (1990). Diffusion-weighted MR imaging of anisotropic water diffusion in cat central nervous system. *Radiology* 176, 439–445.
37. Zhong, J., Petroff, O., Prichard, J., and Gore, J. (1995). Barbiturate-reversible reduction of water diffusion coefficient in flurothyl-induced status epilepticus in rats. *Magn. Reson. Med.* 33, 253–256.
38. Ford, J., Hackney, D., Alsop, D., Jara, H., Joseph, P., Hand, C., and Black, P. (1994). MRI characterization of diffusion coefficients in a rat spinal cord injury model. *Magn. Reson. Med.* 31, 488–494.
39. Duong, T., Sehny, J., Yablonskiy, D., Snider, B., Ackerman, J., and Neil, J. (2001). Extracellular apparent diffusion in rat brain. *Magn. Reson. Med.* 45, 801–810.
40. Silva, M., Omae, T., Helmer, K., Li, F., Fisher, M., and Sotak, C. (2002). Separating changes in the intra- and extracellular water apparent diffusion coefficient following focal cerebral ischemia in the rat brain. *Magn. Reson. Med.* 48, 826–837.
41. Nesic, O., Lee, J., Ye, Z., Unabia, G., Rafati, D., Hulsebosch, C., and Perez-Polo, J. (2006). Acute and chronic changes in aquaporin 4 expression after spinal cord injury. *Neuroscience* 143, 779–792.
42. Lu, H., and Sun, S. (2003). A correlative study between AQP4 expression and the manifestation of DWI after the cervical ischemic brain edema in rats. *Chin. Med. J. (Engl.)* 116, 1063–1069.
43. Guleria, S., Gupta, R., Saksena, S., Chandra, A., Srivastava, R., Husain, M., Rathore, R., and Narayana, P. (2008). Retrograde Wallerian degeneration of cranial corticospinal tracts in cervical spinal cord injury patients using diffusion tensor imaging. *J. Neurosci. Res.* 86, 2271–2280.
44. Zhang, J., Jones, M., DeBoy, C., Reich, D., Farrell, J., Hoffman, P., Griffin, J., Sheikh, K., Miller, M., Mori, S., and Calabresi, P. (2009). Diffusion tensor magnetic resonance imaging of Wallerian degeneration in rat spinal cord after dorsal root axotomy. *J. Neurosci.* 29, 3160–3171.
45. Kim, J., Loy, D., Wang, Q., Budde, M., Schmidt, R., Trinkaus, K., and Song, S. (2010). Diffusion tensor imaging at 3 hours after traumatic spinal cord injury predicts long-term locomotor recovery. *J. Neurotrauma* 27, 587–598.
46. Ellingson, B., Schmit, B., and Kurpad, S. (2010). Lesion growth and degeneration patterns measured using diffusion tensor 9.4-T magnetic resonance imaging in rat spinal cord injury. *J. Neurosurg. Spine* 13, 181–192.
47. Laganà, M., Rovaris, M., Ceccarelli, A., Venturelli, C., Marini, S., and Baselli, G. (2010). DTI parameter optimisation for acquisition at 1.5T: SNR analysis and clinical application. *Comput. Intell. Neurosci.* 2010, 1–8.
48. Mogataadakala, K., and Narayana, P. (2009). In vivo diffusion tensor imaging of thoracic and cervical rat spinal cord at 7 T. *Magn. Reson. Imaging* 27, 1236–1241.
49. Cercignani, M., Horsfield, M., Agosta, F., and Filippi, M. (2003). Sensitivity-encoded diffusion tensor MR imaging of the cervical cord. *AJNR Am. J. Neuroradiol.* 24, 1254–1256.

Address correspondence to:

*Brian D. Schmit, PhD*

*Marquette University*

*Department of Biomedical Engineering*

*PO Box 1881*

*Milwaukee, WI 53201-1881*

*E-mail: brian.schmit@marquette.edu*